Solitary Marangoni-driven convective structures in bistable chemical systems

L. Rongy* and A. De Wit†

Nonlinear Physical Chemistry Unit and Center for Nonlinear Phenomena and Complex Systems, Université Libre de Bruxelles (ULB), CP 231, 1050 Brussels, Belgium

(Received 26 December 2007; published 22 April 2008)

Bistable chemical fronts can be deformed by Marangoni-driven convective flows induced by gradients of surface tension across the front. We investigate here the nonlinear dynamics of such a system by simulations of two-dimensional Navier-Stokes equations coupled to a reaction-diffusion-convection equation for a surface-active chemical species present in the bulk of the solution and involved in a bistable kinetics. We show that Marangoni flows cannot only alter the shape and speed of the front but also change the relative stability of the two stable steady states, reversing in some cases the direction of propagation of the front with regard to the pure reaction-diffusion situation. A detailed parametric study discusses the properties of the asymptotic dynamics as a function of the Marangoni number M and of a kinetic parameter d.

DOI: 10.1103/PhysRevE.77.046310 PACS number(s): 47.15.G−

I. INTRODUCTION

Bistability between two different steady states is a well-known feature of autocatalytic systems. In spatially extended geometries, fronts connecting the two stable steady states can travel with constant shape and speed due to the coupling between reaction and diffusion. The direction and speed of propagation depend on the relative stability of the two stable steady states [1].

Numerous studies have analyzed to what extent advection can influence the dynamics of oscillatory [2–5], excitable [4,6], or bistable reactions [7–9], patterns in reaction-diffusion systems [10,11], and the propagation of combustion fronts in gases [12–16] and of autocatalytic reaction fronts in aqueous solutions [17–23]. Several studies have also analyzed to what extent advection can influence the propagation of traveling bistable wave fronts (see, for instance, [23] and references therein). The main physical effect of the various flows considered (shear, cellular, or percolating flows, time-periodic, turbulent, or chaotic velocity fields) on frontlike solutions is the speedup of the front propagation, with a dependence of the propagation speed on the fluid flow intensity. In these cases, the advection terms result from the presence of an imposed external flow advecting the chemicals, which are thus passive scalars.

However, chemical reactions are also prone to be the motor of convective motions due to density or surface-tension gradients built up across traveling reaction-diffusion fronts. The resulting spatiotemporal dynamics are then the results of a subtle coupling between reactive, diffusive, and convective processes.

Convection corresponding to either buoyancy- [24–28] or surface-tension- [28–32] driven flows across a chemical front has been shown to affect the properties of such fronts in *monostable* systems. For such monostable fronts, the stable steady state of the kinetics invades the unstable one, imposing a unique given direction of propagation. The presence of convection around the front can speed up the front velocity but not change its direction of propagation. For bistable systems, it has been shown that the bistable character of the kinetics can drastically change the nonlinear dynamics of a buoyancy-induced Rayleigh-Taylor instability [33]. Disconnection of droplets of one stable steady state into the other stable state has been observed numerically, a feature absent in the case of a monostable kinetics [27]. The interaction between surface-tension-driven flows (so-called Marangoni flows) and bistable kinetics has, on the other hand, also been the subject of several theoretical works. Using lubrication theory, Dagan and Pismen [34], as well as Dagan and Maldarelli [35], have studied the coupling between Marangoni-driven flows and a bistable chemical reaction occurring at the surface of a thin film, using a one-variable cubic chemical model. Their analyses have shown that a localized chemical wave accompanied by a free surface hydrodynamic flow can develop when insoluble surfactants are subjected to a bistable chemical reaction which maintains two different steady concentration states on the far ends of the film. Bistable chemical reactions occurring only at the surface and involving a single reactant supplied from the bulk have also been studied by Pismen [36], showing the role of Marangoni convection in the stabilization of unstable inhomogeneous states. Pereira *et al.* [37] have further shown using lubrication approximation and a two-variable chemical model that such a coupling can lead to complex dynamics. A limiting assumption of these theories is due to the fact that lubrication equations are valid only if the thickness of the solution layer is much smaller than the characteristic reaction-diffusion length. The presence of sharp concentration gradients across the chemical front thus imposes a limit of validity of lubrication theory, which is restricted to solution films of thickness much smaller than the width of the front. For any solution thickness of the order of the front width, this theoretical approach fails, and one needs to resort to full numerical simulations of the relevant nonlinear model.

Using matched asymptotic expansions to resolve the problem of such sharp interfaces, Pismen [38] has shown that a surface bistable reaction involving insoluble surfactants coupled to Marangoni flows can lead to localized interfacial structures in deeper layers. The Marangoni flows are in

*lrongy@ulb.ac.be
†adewit@ulb.ac.be

this case counteracting the spread of the kinetically more stable state with a higher surface tension. This theoretical approach of the coupling between Marangoni flows and bistable reactions remains, however, restricted to surface reactions. Indeed, as the surfactants are considered as insoluble, the analysis cannot take into account the influence of diffusion of the chemical species in the bulk and hence the important role that transport of the species from the bulk toward the surface can have in the nonlinear dynamics. Moreover, the Marangoni flow induced at the interface will always, by continuity, give rise to a bulk flow, which can interact with the chemical reaction front in a different way in the bulk of the system than at the surface. It is therefore of interest to understand the role played by such bulk motions of the fluid in the existence of localized structures predicted by Pismen [38].

In this context, the objective of the present paper is to analyze asymptotic dynamics resulting from the coupling between bistable kinetics occurring in the bulk of a two-dimensional layer of fluid and Marangoni-driven flows. Our goal is to understand to what extent internal chemically driven flows arising from gradients of surface tension across the bistable chemical front affect the spatiotemporal dynamics of the system. To do so, we numerically integrate the incompressible Navier-Stokes equations in a two-dimensional system and couple via a Marangoni boundary condition the flow evolution to that of a surface-active chemical species present in the bulk and subject to a bistable kinetics. We show that a bistable propagating front can be deformed both at the surface and in the bulk due to convective flows. Furthermore, the front can be stopped and can even see its direction of propagation reversed because of the competition with these Marangoni effects. An inhomogeneous stationary state can then be achieved within a finite parametric domain and the relative stability of the two kinetically stable steady states can be drastically affected.

In this context, the paper is organized as follows. In Sec. II, we summarize the model system and discuss the corresponding dimensionless equations describing the dynamics. The relevant dimensionless parameters of the problem, i.e., a solutal Marangoni number M and a kinetic parameter d, are introduced. In Sec. III, we describe the nonlinear dynamics of the system and discuss the important properties of the front evolution in the (M,d) parameter plane. Eventually, conclusions are drawn in Sec. IV.

II. MODEL SYSTEM

Our model closely follows the one we developed previously to analyze Marangoni effects on traveling monostable fronts [31,32]. Indeed we consider a two-dimensional (2D) thin aqueous solution layer of dimensionless length L_x and height L_z in which an isothermal planar chemical front producing a surface-active product of concentration c propagates along the x direction. The surface tension of the solution depends on c but the surface is assumed to be nondeformable and there is no evaporation so that we do not address the dynamics in the air layer. The solution density and viscosity are taken constant in space and time. Dimensionless units constructed upon the characteristic reaction-diffusion scales are used, i.e., for time, $\tau_c=1/ka_0^2$, for length, $L_c=\sqrt{D\tau_c}$, for velocity, $U_c=\sqrt{D/\tau_c}$, for pressure, $p_c=\mu/\tau_c$, and for concentration, a_0, with k the rate constant of the autocatalytic reaction, a_0 the initial reactant concentration, D the molecular diffusion coefficient of the product, and μ the fluid viscosity. The dimensionless evolution equations for the 2D flow field $\underline{v}=(u,w)$ and the concentration c read

$$\frac{\partial c}{\partial t}+\underline{v}\cdot\underline{\nabla}c=\nabla^2 c+c(1-c)(c-d), \tag{1}$$

$$\frac{\partial \underline{v}}{\partial t}+\underline{v}\cdot\underline{\nabla}\underline{v}=S_c\cdot(-\underline{\nabla}p+\nabla^2\underline{v}), \tag{2}$$

$$\mathrm{div}\ \underline{v}=0 \tag{3}$$

with $0<d<1$ being a kinetic parameter and $S_c=\nu/D$ the Schmidt number of the problem, where $\nu=\mu/\rho_0$ is the kinematic viscosity and ρ_0 is the density of the solution. The rectangular system has rigid sidewalls at $x=0$ and L_x, a rigid bottom at $z=0$, and a free upper surface at $z=L_z$. At each boundary of this domain we require zero-flux boundary conditions for the chemical concentration c. The hydrodynamic boundary conditions at the rigid boundaries are no-slip conditions $u=0$ and $w=0$. At the free surface $(z=L_z)$, we require $w=0$ and use a Marangoni boundary condition for the horizontal fluid velocity u to include the changes in surface tension induced by the concentration gradient of the surface-active product across the front, i.e.,

$$\frac{\partial u}{\partial z}=-M\frac{\partial c}{\partial x}. \tag{4}$$

This condition (4) introduces the dimensionless solutal Marangoni number M defined as

$$M=\frac{-1}{\mu\sqrt{Dk}}\frac{d\gamma}{dc}, \tag{5}$$

which is positive (negative) if the surface-active product decreases (increases) the surface tension γ. As the characteristic scales of the nondimensionalization are here the typical scales of the reaction-diffusion (RD) system, the Marangoni number is inversely proportional to the square root of the kinetic constant k of the chemical reaction. This number M quantifies the coupling strength between the hydrodynamic motions and the RD processes. The two key parameters of the problem are here M and d.

The initial condition corresponds to a planar RD front propagating in a solution in the absence of any fluid flow. The initial fluid velocity and the hydrostatic pressure gradient are thus set to zero everywhere in the system. The initial condition for the surface-active product concentration is the convectionless RD profile, solution of the RD problem

$$\frac{\partial c}{\partial t}=\nabla^2 c+c(1-c)(c-d). \tag{6}$$

The advantage of the simple bistable kinetics $c(1-c)(c-d)$ is to allow us to obtain an analytical expression of the RD front

connecting the two stable steady states (SSSs) $c=0$ and 1. We choose here to start with the steady states $c=1$ and 0 to be located, respectively, to the left and to the right of the initial location of the front, i.e., we impose that the solution satisfies $c=1$ when $x\to-\infty$ and $c=0$ for $x\to+\infty$. Explicitly, the front solution reads then

$$c(x,t)=\frac{1}{1+e^{(x-vt)/\sqrt{2}}}=\frac{1}{2}\left[1+\tanh\left(-\frac{\sqrt{2}}{4}(x-vt)\right)\right], \quad (7)$$

where $v=\frac{\sqrt{2}}{2}(1-2d)$ is the constant RD speed of the front [1]. Solution (7) provides an analytical expression to be recovered in the limit $M\to 0$ allowing us thus to test convergence results [34] for small values of M. The relative stability of the two SSSs depends on d. When $d<0.5$, $c=1$ is the most stable steady state invading $c=0$, the reverse being observed for $d>0.5$. For the unique value $d=0.5$, the two SSSs are equistable and the front has no RD propagation speed, i.e., $v=0$. The front remains then at its initial position. From Eq. (7), it is seen that the width w_{RD} of this front, arbitrarily defined as the distance between $c=0.99$ and 0.01, equals $w_{\mathrm{RD}}=2\sqrt{2}\ln 99=13$.

The goal of this paper is to analyze to what extent Marangoni-driven flows will affect the relative stability of the two SSSs as a function of both parameters M and d. To do so, we numerically integrate Eqs. (1)–(3) by finite-difference methods [31]. We use a semi-implicit projection method to solve Eqs. (2) and (3). The code has been validated through comparison with known analytical results [31]. In addition to the tests described in our previous study, we numerically reproduce the planar RD front (7) with the correct width and speed v for different values of d when the Marangoni number M is equal to zero.

III. 2D MARANGONI FLOW AROUND BISTABLE CHEMICAL FRONTS: NONLINEAR DYNAMICS

Our model includes five dimensionless parameters: one kinetic parameter d, two hydrodynamic parameters, i.e., the Marangoni number M and the Schmidt number S_c, and two geometric parameters, which are the length L_x and height L_z of the system. The length L_x does not influence the results as long as it is taken sufficiently long for the front not to interact with a lateral boundary on the time of interest. Typical Schmidt numbers for aqueous solutions run between 500 and 1500 [31], a range in which the numerical results are quantitatively the same, which means that we effectively analyze a Stokes flow. We fix here $S_c=1500$. We consider a quite thin layer of 1 mm in thickness, which is more or less the width of an autocatalytic chemical front [39]. In dimensionless variables, we take then $L_z=10$ since the dimensionless width of the RD front $w_{\mathrm{RD}}\approx 13$. The Marangoni number, quantifying the coupling between hydrodynamics and RD processes, and d, determining the relative stability of the two SSSs, are the two key parameters of our model and will be varied throughout the remainder of this article.

The initial condition corresponds to a planar reaction-diffusion front propagating at the constant RD speed v in the solution where there is initially no fluid flow. When $M=0$, no hydrodynamic motion appears in the solution and the planar front propagates without any deformation at its constant propagation speed v. When the Marangoni number differs from zero, convection is initiated at the surface due to the surface tension gradient across the front. This surface flow is directed toward the region of larger surface tension. Following this initial acceleration at the surface, a bulk flow is induced in the opposite direction because the fluid is incompressible and flows in a bounded system. Let us recall that, in our choice of initial condition, $c=1$ is at the left side of the system while $c=0$ is at its right. For positive M, the concentration of the product c decreases the surface tension and leads therefore to a positive fluid velocity at the surface, directed to the right toward the region of $c=0$. Conversely, for negative M, we get a negative surface flow directed to the left.

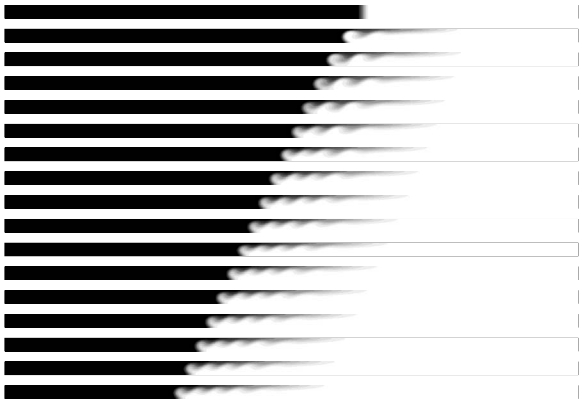

FIG. 1. Propagation of a chemical front separating two equistable steady states ($d=0.5$) in the presence of chemically induced Marangoni convection for $M=500$, shown from top to bottom from $t=0$ up to 80 with a time interval of $\Delta t=5$. The aspect ratio between $L_x=400$ and $L_z=10$ is preserved.

A. Equistable steady states

Let us first consider the situation where the two SSSs $c=0$ and 1 are equistable, i.e., when $d=0.5$. In the absence of any flow, the RD propagation speed v of the front connecting the two SSSs is therefore equal to zero. The base state is thus an immobile RD front for $M=0$. As soon as Marangoni effects are switched on, convection sets in, deforming the front, which starts to move entrained by the convective flows. Figure 1 shows two-dimensional density plots of the concentration ranging from $c=0$ (white) to 1 (black) for increasing time, with $d=0.5$ and a positive Marangoni number $M=500$. The front is observed to move globally to the left even if the acceleration at the surface is to the right. The effect of Marangoni convection on this initially immobile RD front results in a deformation of the planar front as for the monostable kinetics [31] but what is particular here is the direction of motion of the front. Even if the two steady states are kinetically equistable, the front propagates to the left as if the Marangoni convection modified the relative stability of the two steady states and made the one with the largest surface tension ($c=0$) more stable. Several convection rolls de-

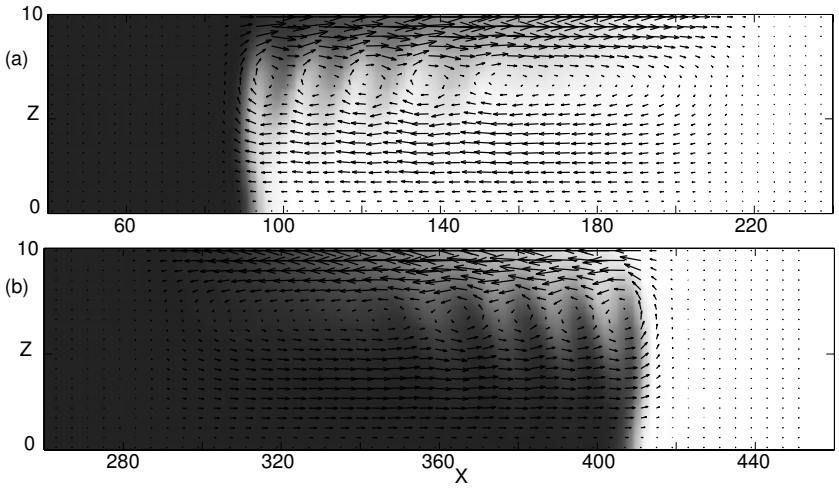

FIG. 2. Focus on the asymptotic multicellular fluid flow traveling with the deformed front for $d=0.5$, $M=$ (a) 500 and (b) −500. The two structures shown at $t=100$ are symmetric with regard to the initial position of the front located at $x_{in}=250$. The z direction has been magnified in order to see the details of the velocity field.

velop across the layer, leading to oscillations of the concentration field. After around $50\tau_c$, the system has reached an asymptotic regime in which the front propagates at a constant speed V and the oscillating front shape and fluid velocity field remain invariant in the comoving frame traveling at speed V. The steady traveling flow field is localized in the region of the deformed front and can be visualized in Fig. 2(a). Figure 2(b) shows the asymptotic fluid flow and concentration field for $M=-500$. We can see that the dynamics at negative M can be obtained by symmetry from the situation with corresponding positive M of the same magnitude according to the transformation $c(x_{in}+x)\rightarrow 1-c(x_{in}-x)$, $u(x_{in}+x)\rightarrow -u(x_{in}-x)$, and $w(x_{in}+x)\rightarrow w(x_{in}-x)$, where x_{in} is the initial position of the front.

B. Influence of the Marangoni number

In order to quantify the effect of Marangoni convection on the front propagation, we next characterize the deformation of the front, the constant propagation speed V, and the maximum horizontal fluid velocity u_{max} as functions of M in the asymptotic regime. The deformation of the front can be quantified by a mixing length defined as the distance between $\langle c(x,t)\rangle=0.01$ and $\langle c(x,t)\rangle=0.99$, i.e., between the tip and the rear of the transversed averaged profile,

$$\langle c(x,t)\rangle = \frac{1}{L_z}\int_0^{L_z} c(x,z,t)dz. \tag{8}$$

For each value of the Marangoni number scanned here ($-500\leq M\leq 500$), the dynamics of the system always reaches an asymptotic regime but the time needed to achieve it increases with $|M|$. On short times, the mixing length increases [31], indicating an initial rise of the front deformation during which convection sets in. The mixing length next saturates in the asymptotic regime to a constant value W plotted as a function of M in Fig. 3(a). It is seen that W is symmetric between negative and positive M and increases with $|M|$, i.e., with the intensity of the surface tension gradient across the front. For $M=0$, we recover $W=13$, i.e., the width of the RD front. Figure 3(b) represents the constant propagation speed V of the asymptotic localized structure, obtained by measuring the slope of the position of the tip of

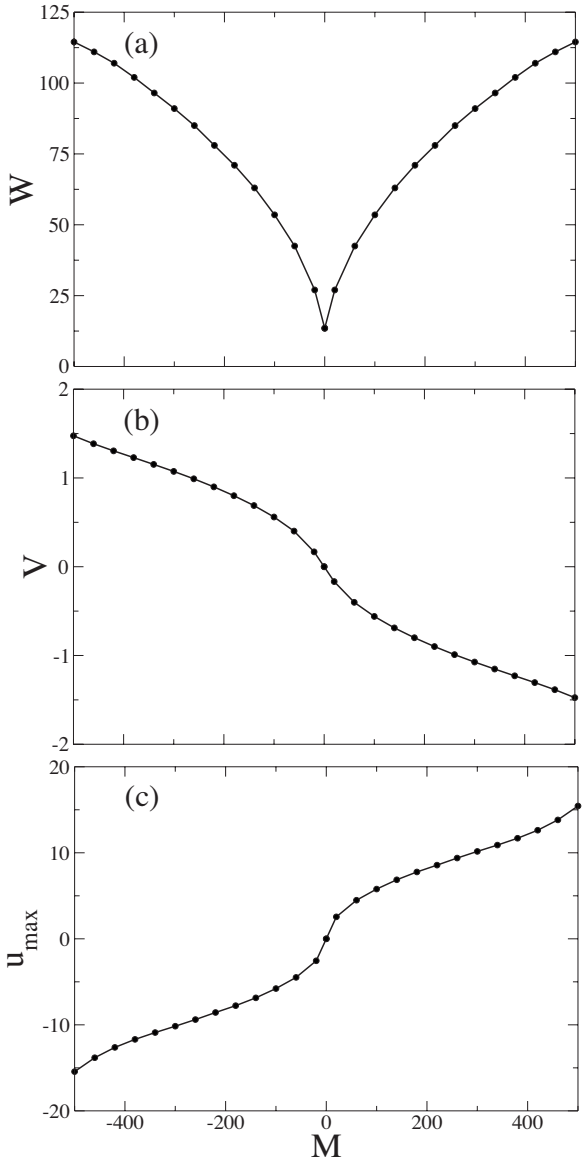

FIG. 3. Asymptotic mixing length W (a), propagation speed V (b), and maximum horizontal fluid velocity u_{max} (c) as a function of the Marangoni number for $d=0.5$.

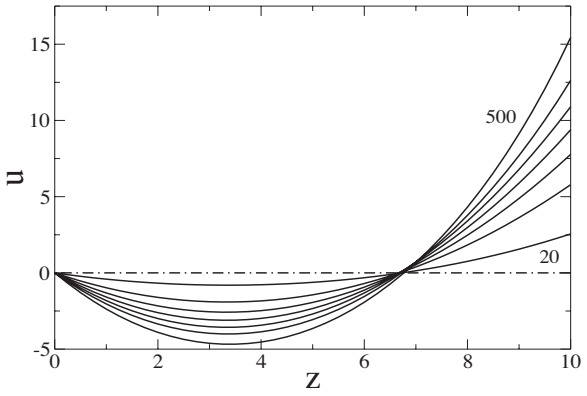

FIG. 4. Asymptotic profiles of the horizontal fluid velocity u across the layer at $x_{max}=x_{u=u_{max}}$ for $d=0.5$ and increasing positive Marangoni numbers between 20 and 500 with an interval of 80 between two successive curves. The dot-dashed curve corresponds to $M=0$ when there is no convection.

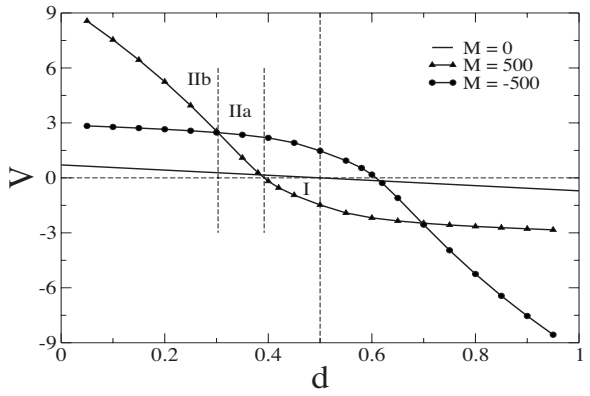

FIG. 5. Asymptotic propagation speed V as a function of d for $M=\pm 500$, compared with the propagation speed of the RD front.

the front as a function of time. For positive M, the flow at the surface is toward the right but nevertheless the bulk return flow globally entrains the deformed front to the left and hence V is negative. The reverse is true for negative M. Figure 3(c) shows the horizontal fluid velocity u of maximum intensity u_{max} as a function of M. This value is always located at the surface and is therefore positive for $M>0$ even if globally $V<0$. In Fig. 2(a), for example, u_{max} is located at $x=135$, $z=10$. We note that both $|V|$ and $|u_{max}|$ increase with $|M|$, their respective values for $M>0$ and $M<0$ being antisymmetric with regard to $M=0$, where the RD speed v (here equal to zero for $d=0.5$) is recovered. For $|M|=500$, the flow is characterized by the presence of several vortices inside the front as seen in Fig. 2. The number of vortices increases with M. This can be compared to the hydrothermal waves obtained in the case of thermocapillary convection in a planar liquid layer with a horizontal temperature gradient [40,41]. When the Marangoni number is increased above the instability threshold in that system, the basic return flow loses its stability and the motion becomes oscillatory with a multicellular flow. The hydrothermal waves propagate toward the hot wall of the layer, i.e., toward the region of lower surface tension as in our case. We also observe here a multicellular flow above a certain critical Marangoni number but the main different feature is the fact that the multicellular flow is here localized in space and propagates at a constant speed but does not oscillate in time. This is due to the fact that the surface tension gradient is localized here across the chemical front (see Fig. 2). A more detailed discussion of these oscillations is presented in Sec. III D as a function of M and d. Lastly, we have plotted in Fig. 4 vertical profiles of the horizontal fluid velocity u at the horizontal location x_{max} where u is maximum for the various positive M. Those profiles show that $u(x_{max},z)$ has all the properties of a return flow [40–42], getting its minimum and maximum values at, respectively, $z=L_z/3$ and L_z for each M, and being equal to zero at $z=2L_z/3$.

Since the convection affects the relative stability of the two steady states when they are equistable, we have next modified the value of d between 0 and 1 to see how Marangoni convection affects the relative stability of the two SSSs in general.

C. Influence of the kinetic parameter d

For each pair of (M,d) values we have considered, the coupling between a bistable chemical front and chemically induced Marangoni convection gives rise after a transient to an asymptotic steady dynamics characterized by a deformed front propagating at a constant speed V and surrounded by a localized steady fluid flow. The system presents a symmetry between positive and negative M according to the following transformation: $M\rightarrow -M$, $d\rightarrow 1-d$, $c(x_{in}+x)\rightarrow 1-c(x_{in}-x)$, $u(x_{in}+x)\rightarrow -u(x_{in}-x)$, $w(x_{in}+x)\rightarrow w(x_{in}-x)$ and the asymptotic properties $W\rightarrow W$, $V\rightarrow -V$, and $u_{max}\rightarrow -u_{max}$.

Let us first consider the influence of d on the system dynamics at a constant M. Figure 5 compares the asymptotic propagation speed V at $M=\pm 500$ to the RD speed v for various values of d. In the absence of flow ($M=0$), let us recall that the RD speed $v=\frac{\sqrt{2}}{2}(1-2d)$ is positive (negative) for $d<0.5$ ($d>0.5$), meaning that the front travels then to the right (left). Three key regions can be identified in Fig. 5 when Marangoni effects are at play: regions I, IIa, and IIb, the rest of the figure being symmetric with regard to $d=0.5$. The most striking feature is in region I ($0.392\leq d\leq 0.5$ for $M=500$), where the stability of the two steady states is inverted by Marangoni convection for positive M. Indeed, as $d<0.5$, $c=1$ is the most stable steady state of the chemical kinetics and the propagation speed of the front should be positive, with $c=1$ invading $c=0$. However, as we have seen in the previous section with equistable steady states, the Marangoni effect tends to confer a negative propagation speed V on the front for positive M. The stability inversion in region I is therefore the result of the competition between those two antagonistic trends with the Marangoni effect winning over the RD trend. However, as d decreases at fixed M, the chemical driving force grows as the kinetic stability difference between the two steady states increases. Eventually, there is a value of d (here $d\approx 0.392$) for which the propagation of the front is stopped.

In regions IIa and IIb, the competition between the chemical and the Marangoni convective driving forces is in favor of the chemical force, since the propagation speed V is posi-

tive again just like the RD speed v. Nevertheless, we can still differentiate between the two regions. In region IIa ($0.303 \leq d \leq 0.392$), the propagation speed for positive M is smaller than for negative M. Since a Marangoni flow with negative M tends to confer a positive propagation speed on the front, it reinforces the chemical driving force, which explains the behavior in region IIa. Let us note some characteristics of the positive M curve in this region. For $0.385 < d \leq 0.392$, Marangoni convection slows down the front propagation compared to the reaction-diffusion speed, which is rather rare, since convection-enhanced mass transport usually increases the front propagation speed. At $d=0.385$, Marangoni convection does not affect the propagation speed at all ($V=v$), while at $d=0.303$, the propagation speed does not depend on the direction of the surface tension gradient, as the speed V is the same for both $M=500$ and $M=-500$.

Finally, let us consider region IIb, where the propagation speed for positive M is now larger than for negative M. Another mechanism has to come into play to explain here the results between positive and negative M. The results for the monostable kinetics obtained in our previous study [31] are situated in this region since they correspond to $d=0$. When $M>0$, the flow at the surface is in the same direction as the front propagation, so that we expect the reaction-diffusion-convection propagation speed V and the mixing length W to be larger than for negative M, due to a cooperative phenomenon at the surface where the fluid flow is initiated. On the other hand, if the front is more deformed, the surface tension gradient is weaker, and hence the intensity of $u_{\max}$ is smaller than for negative M. These are the results we observed for the monostable kinetics and which are coherent with the ones observed in region IIb. In Figs. 6(a) and 6(b) we observe that the asymptotic mixing length W and the maximum intensity of the horizontal velocity $|u_{\max}|$ follow this explanation in regions I, IIa, and IIb, while it is only true in region IIb for the propagation speed.

The horizontal velocity profiles across the layer, $u(x_{\max},z)$, have approximately the same return flow structure for each value of d and M [see Fig. 6(c) with $M=500$ for example]. Figure 7 shows the three properties characterizing the asymptotic dynamics as a function of d for $M=100$, 300, and 500. The detailed explanation given above for the propagation speed behavior at $M=500$ is valid for each M we have studied as seen in Fig. 7(b). However, the value of d for which $V=0$ is logically shifted toward $d=0.5$ as M decreases since the opposing Marangoni effect is then weakening. The asymptotic mixing length W is a monotonically decreasing function of d, while the maximum horizontal fluid velocity $u_{\max}$ presents a minimum. At every constant value of M, the time needed to reach the asymptotic regime is a simple function of d presenting one maximum $d_{\max}$. For values of d around this maximum, the time needed to reach the steady regime increases with M, while it is independent of M otherwise. Let us note that $d_{\max}$ is very close to the value of d for which $u_{\max}$ is minimum and the propagation speed is zero.

Figure 7(c) shows that the convection is minimum when the propagation speed of the asymptotic structure is zero. At this particular value of d, let us call it d_0, the different effects compensate exactly to stop the front, so that we expect the surface tension gradient to have the smallest effect on the system and hence the smallest $u_{\max}$. On each side of d_0, V and $u_{\max}$ increase, indicating that the Marangoni effect has a stronger influence on the system when the stability difference between the two steady states increases. On the other hand, this observation is true for the mixing length only for $d < d_0$.

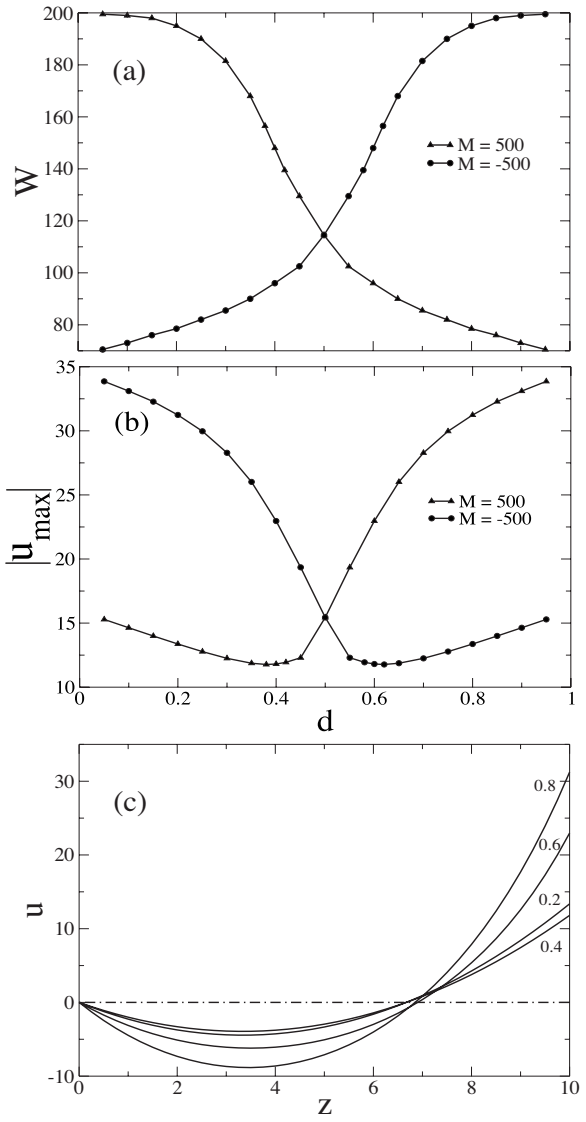

FIG. 6. Asymptotic mixing length W (a) and intensity of the maximum horizontal fluid velocity $|u_{\max}|$ (b) as a function of d for $M=\pm 500$. (c) Asymptotic profiles of the horizontal fluid velocity u across the layer at $x_{\max}$ for various d at $M=500$.

Figure 8 shows that the asymptotic mixing length W, the intensity of the propagation speed V, and the maximum horizontal fluid velocity $u_{\max}$ all increase with M for each value of d. Indeed, when M increases, the surface tension gradient increases across the front, giving rise to more important Marangoni convection, and hence a more important deformation of the front and propagation speed. This result concerning the propagation speed of the front is similar to what was observed in reaction-diffusion-advection systems where the front is sped up by fluid advection and its propagation speed

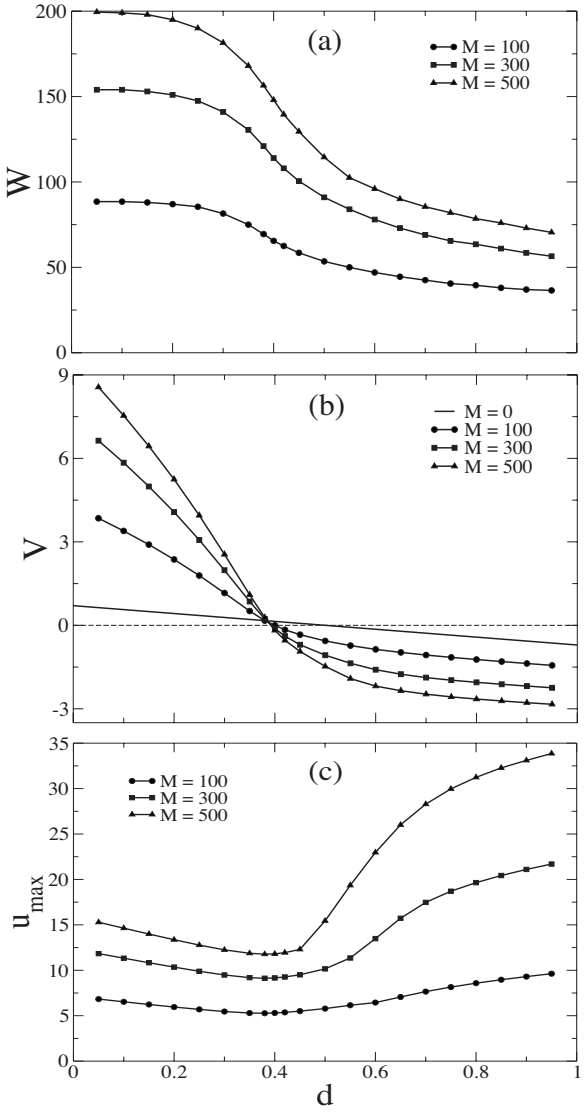

FIG. 7. Asymptotic mixing length W (a), propagation speed V (b), and maximum horizontal fluid velocity u_{max} (c) as a function of d for various M.

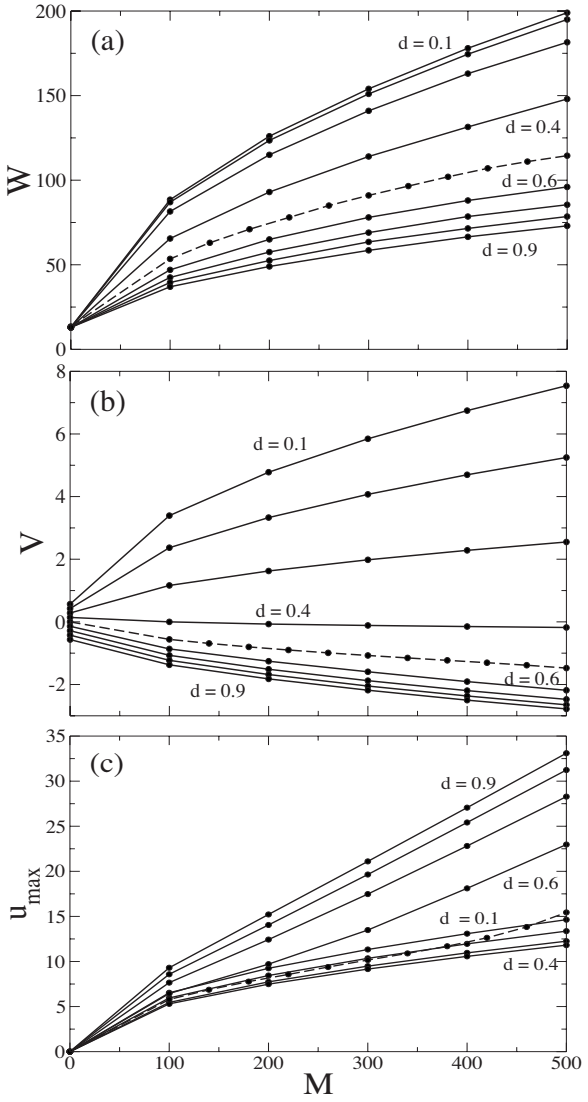

FIG. 8. Asymptotic mixing length W (a), propagation speed V (b), and maximum horizontal fluid velocity u_{max} (c) as a function of M for increasing d between 0.1 and 0.4, and between 0.6 and 0.9, with an interval of 0.1 between two successive curves. The dashed lines correspond to $d=0.5$.

increases with the flow intensity [13–15,18–22]. There is, however, a major difference in the fact that here chemistry is not slaved to the flow. The nonlinear pattern results here from a subtle interplay between reaction, diffusion, and chemically driven convection processes. The maximum velocity of the front is thus not imposed by the given flow field properties but is set by the Marangoni number characterizing the amplitude of the response of the flow to concentration gradients.

D. Multicellular flow

An interesting property of the dynamics resulting from the interaction between a bistable kinetics and chemically induced Marangoni convection is the existence of a multicellular flow traveling with the front and leading to spatial oscillations of the concentration field. This asymptotic structure propagates at a constant speed and remains steady in the comoving frame for certain values of d. Those oscillations of the concentration and flow fields had already been observed in our previous study with monostable kinetics for $M \geq 220$ but always in a transient way [31]. Here, on the other hand, they are maintained in the asymptotic dynamics for $d \geq 0.5$ at large M (see Fig. 1). The concentration oscillations are less pronounced and the number of flow vortices decreases when d increases from 0.5. On the other hand, for a fixed d, the intensity and number of steady oscillations increase with M, while they are difficult to observe at small M.

At the other limit, for $d \leq 0.3$, the multicellular flow and concentration oscillations are only transient (see Fig. 9 for $d=0.3$, $M=500$). For any fixed M, the number of vortices increases at short times, but they disappear in favor of one steady convection roll propagating with the deformed front without oscillations, which corresponds to the asymptotic structure we have characterized for the monostable kinetics

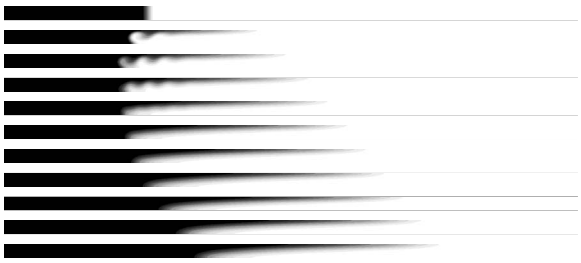

FIG. 9. Propagation of a chemical front presenting transient oscillations that disappear after $(25-30)\tau_c$ ($d=0.3$) due to chemically induced Marangoni convection for $M=500$. The dynamics is shown from top to bottom from $t=0$ to 50 with a time interval of $\Delta t=5$. The aspect ratio between $L_x=400$ and $L_z=10$ is preserved.

[31]. At a constant $d \leq 0.3$, the intensity of the transient oscillations increases with the Marangoni number, but they disappear at roughly the same time [after $(25-30)\tau_c$ for $d=0.3$]. On the other hand, the transient oscillations disappear later and are more pronounced when d increases in the range $0 \leq d \leq 0.3$.

The transition between transient and steady oscillations is not easy to determine but occurs in the range $0.3 < d < 0.5$. Indeed, for those values of d, strong oscillations in the concentration and flow field initially appear, but they almost disappear after some time without completely resorbing. We believe that the transition should appear around d_0 where the propagation speed is zero.

In conclusion, the concentration and velocity oscillations are steady when the surface fluid flow is opposing the front propagation, while they are transient when the flow induced at the surface is parallel to the propagation direction. The latter corresponds to the results obtained with the monostable kinetics. However, it is important to notice that, in that case, when the surface fluid flow is opposing the front propagation, a steady additional deformation of the front occurs, which increases with $|M|$, but there is no steady oscillation as for the bistable kinetics. Finally, the increase in intensity of the oscillations when d gets closer to d_0, for both the steady and the transient dynamics, is probably due to the fact that they can develop more if the front propagates more slowly.

IV. CONCLUSIONS

Bistable fronts connect in space two stable steady states and travel at a constant reaction-diffusion speed v depending on the relative stability of these two states. To get insight into the question of how such fronts can be affected by surface-tension driven flows, we have numerically integrated Navier-Stokes equations on a 2D domain with a Marangoni boundary condition at a free surface coupled to the evolution equation of a surface-active product present in the bulk and involved in a bistable kinetics. We have shown that Marangoni-driven flows resulting from surface tension gradients across such fronts have a profound influence on the dynamics of these fronts. First of all, they lead to a spatial deformation of the front due to the presence of convective flows generated at the surface by the Marangoni acceleration and extending in the bulk. These flows induce an increase of the overall speed of the front, this speed being usually larger in absolute value than the reaction-diffusion speed v independently of the direction of the Marangoni flows at the surface. Such results are similar to those that have been observed in the case of monostable fronts [31,32].

The bistable case presents, however, a strong difference with the monostable case: Marangoni flows are able to change the relative stability of the two bistable states. In the case of monostable fronts, Marangoni effects can accelerate traveling fronts with the clockwise or anticlockwise character of the vortex depending on the sign of the Marangoni number, but its direction of propagation always remaining such that the stable steady state invades the unstable one. For bistable systems, the Marangoni effects are on the contrary much more striking: fronts deformed by Marangoni flows are still able to travel more quickly than in the RD case, but more strikingly they can also reverse their direction of propagation when surface tension effects are added. A parametric study of the properties of such convective fronts in the (M,d) parameter plane has identified regimes in which the Marangoni effects can either maintain the preferred RD direction of propagation or, on the contrary, reverse it. For one specific value of d depending on M, the front can remain stationary even when the RD speed is nonzero. The dependence on d and M of the asymptotic propagation speed V and mixing length W and of the maximum horizontal fluid velocity $u_{\max}$ have also been discussed.

Our results confirm that the solitary structures due to the competition between interfacial bistable reactions and Marangoni flow predicted by Pismen [38] also exist when the chemical reaction takes place in the bulk of the solution layer. This is not intuitive since, if the Marangoni flow is opposing the RD front direction of propagation at the surface, it means that in a large part of the bulk [two-thirds of the layer; cf. Fig. 6(c) for instance] they are going in the same direction. Consequently, the overall direction of the reaction-diffusion-convection structure cannot be predicted by considering the forces at the surface but is the result of a much more complex interaction between RD processes and Marangoni effects. We have characterized the dynamics of deformation of the front in this bulk in details. The interest of our results is furthermore to isolate peculiar limiting cases which could be the starting point for more analytical insights into nonlinear reaction-diffusion-convection dynamics. A first limit is the one for $d=1/2$. In that case, the reaction-diffusion base state has a propagation speed equal to zero, which should facilitate theoretical analytical expansions in small M or analysis of the limit for large M to get insight into the scaling properties of the reaction-diffusion-convection asymptotic dynamics induced by Marangoni effects. Another limit of interest is the one for which the convectively deformed front has now a zero speed as well, resulting from an antagonistic combination of reaction-diffusion dynamics traveling in one given direction and Marangoni flows that are pushing the front on average in the other direction. In that case, the asymptotic dynamics is stationary in the laboratory reference frame, which should favor development of analytical insights into nonlinear Marangoni-driven localized reaction-diffusion-convection patterns.

ACKNOWLEDGMENTS

Discussions with P. Colinet, P. Borckmans, A. Zebib, and G. M. Homsy are gratefully acknowledged. L.R. is supported by the FNRS (Belgium). A.D. acknowledges financial support from Prodex (Belgium), FNRS, and the "Communauté Française de Belgique" ("Actions de Recherches Concertées" program).

[1] J. D. Murray, *Mathematical Biology* (Springer, Berlin, 2002).
[2] Z. Neufeld, I. Z. Kiss, C. Zhou, and J. Kurths, Phys. Rev. Lett. **91**, 084101 (2003).
[3] C. R. Nugent, W. M. Quarles, and T. H. Solomon, Phys. Rev. Lett. **93**, 218301 (2004).
[4] M. S. Paoletti and T. H. Solomon, Europhys. Lett. **69**, 819 (2005).
[5] V. Pérez-Muñuzuri, Phys. Rev. E **73**, 066213 (2006).
[6] V. Pérez-Muñuzuri and G. Fernández-García, Phys. Rev. E **75**, 046209 (2007).
[7] Q. Ouyang, V. Castets, J. Boissonade, J. C. Roux, P. De Kepper, and H. L. Swinney, J. Chem. Phys. **95**, 351 (1991).
[8] S. N. Menon and G. A. Gottwald, Phys. Rev. E **71**, 066201 (2005).
[9] S. M. Cox, Phys. Rev. E **74**, 056206 (2006).
[10] P. Andresén, M. Bache, E. Mosekilde, G. Dewel, and P. Borckmans, Phys. Rev. E **60**, 297 (1999); **62**, 2992 (2000).
[11] M. Kaern and M. Menzinger, Phys. Rev. E **60**, R3471 (1999).
[12] V. Yakhot, Combust. Sci. Technol. **60**, 191 (1988).
[13] P. F. Embid, A. Majda, and P. Souganidis, Combust. Sci. Technol. **103**, 85 (1994).
[14] P. Constantin, A. Kiselev, A. Oberman, and L. Ryzhik, Arch. Ration. Mech. Anal. **154**, 53 (2000).
[15] M. Abel, A. Celani, D. Vergni, and A. Vulpiani, Phys. Rev. E **64**, 046307 (2001).
[16] I. Z. Kiss, J. H. Merkin, S. K. Scott, P. L. Simon, S. Kalliadasis, and Z. Neufeld, Physica D **176**, 67 (2003).
[17] P. D. Ronney, B. D. Haslam, and N. O. Rhys, Phys. Rev. Lett. **74**, 3804 (1995).
[18] M. A. Allen, J. Brindley, J. H. Merkin, and M. J. Pilling, Phys. Rev. E **54**, 2140 (1996).
[19] B. F. Edwards, Phys. Rev. Lett. **89**, 104501 (2002).
[20] M. Leconte, J. Martin, N. Rakotomalala, and D. Salin, Phys. Rev. Lett. **90**, 128302 (2003).
[21] S. M. Cox and G. A. Gottwald, Physica D **216**, 307 (2006).
[22] A. Pocheau and F. Harambat, Phys. Rev. E **73**, 065304(R) (2006).
[23] Z.-C. Wang, W.-T. Li, and S. Ruan, J. Differ. Equations **238**, 153 (2007).
[24] L. Rongy, N. Goyal, E. Meiburg, and A. De Wit, J. Chem. Phys. **127**, 114710 (2007).
[25] M. Böckmann and S. C. Müller, Phys. Rev. E **70**, 046302 (2004).
[26] D. Horváth, T. Bánsági, Jr., and A. Tóth, J. Chem. Phys. **117**, 4399 (2002).
[27] A. De Wit, Phys. Fluids **16**, 163 (2004).
[28] Y. Shi and K. Eckert, Chem. Eng. Sci. **61**, 5523 (2006).
[29] S. Kai, T. Ariyoshi, S. Inenaga, and H. Miike, Physica D **84**, 269 (1995).
[30] H. Kitahata, R. Aihara, N. Magome, and K. Yoshikawa, J. Chem. Phys. **116**, 5666 (2002).
[31] L. Rongy and A. De Wit, J. Chem. Phys. **124**, 164705 (2006).
[32] L. Rongy and A. De Wit, J. Eng. Math. **59**, 221 (2007).
[33] A. De Wit, P. De Kepper, K. Benyaich, G. Dewel, and P. Borckmans, Chem. Eng. Sci. **58**, 4823 (2003).
[34] Z. Dagan and L. M. Pismen, J. Colloid Interface Sci. **99**, 215 (1984).
[35] Z. Dagan and C. Maldarelli, Chem. Eng. Sci. **42**, 1259 (1987).
[36] L. M. Pismen, J. Colloid Interface Sci. **102**, 237 (1984).
[37] A. Pereira, P. M. J. Trevelyan, U. Thiele, and S. Kalliadasis, Phys. Fluids **19**, 112102 (2007).
[38] L. M. Pismen, Phys. Rev. Lett. **78**, 382 (1997).
[39] A. Hanna, A. Saul, and K. Showalter, J. Am. Chem. Soc. **104**, 3838 (1982).
[40] M. K. Smith and S. H. Davis, J. Fluid Mech. **132**, 119 (1983).
[41] J. Xu and A. Zebib, J. Fluid Mech. **364**, 187 (1998).
[42] A. A. Nepomnyashchy, M. G. Velarde, and P. Colinet, *Interfacial Phenomena and Convection* (Chapman and Hall/CRC, Boca Raton, FL, 2002).